A method for predicting city-wide electricity gains from photovoltaic panels based on LiDAR and GIS data combined with hourly Daysim Simulations

Authors:
J. Alstan Jakubiec[1]
Christoph F. Reinhart[1]

1. Building Technology Program, Massachusetts Institute of Technology, Cambridge, MA

Abstract

In this paper we present, demonstrate and validate a method for predicting city-wide electricity gains from photovoltaic panels based on detailed 3D urban massing models combined with Daysim-based hourly irradiation simulations, typical meteorological year climactic data and hourly calculated rooftop temperatures. The resulting data can be combined with online mapping technologies and search engines as well as a financial module that provides building owners interested in installing a photovoltaic system on their rooftop with meaningful data regarding spatial placement, system size, installation costs and financial payback. As a proof of concept, a photovoltaic potential map for the city of Cambridge, Massachusetts, USA, consisting of over 17,000 rooftops has been implemented as of September 2012.

The new method constitutes the first linking of increasingly available GIS and LiDAR urban datasets with the validated building performance simulation engine Daysim, thus-far used primarily at the scale of individual buildings or small urban neighborhoods. A comparison of the new method with its predecessors reveals significant benefits as it produces hourly point irradiation data, supports better geometric accuracy, considers reflections from neareby urban context and uses predicted rooftop temperatures to calculate hourly PV efficiency. A validation study of measured and simulated electricity yields from two rooftop PV installations in Cambridge shows that the new method is able to predict annual electricity gains within 3.6 to 5.3% of measured production when calibrating for actual weather data and detailed PV panel geometry. This predicted annual error using the new method is shown to be less than the variance which can be expected from climactic variation between years. Furthermore, because the new method generates hourly data, it can be applied to peak load mitigation studies at the urban level. This study also compares predicted monthly energy yields using the new method to those of preceding methods for the two validated test installations and on an annual basis for ten buildings selected randomly from the Cambridge dataset.

A version of this paper is published in:

Solar Energy 93 (C), 2013. doi:10.1016/j.solener.2013.03.022

Please cite this paper as:

Jakubiec, J. A., Reinhart, C. F. (2012). A method for predicting city-wide electric production from photovoltaic panels based on LiDAR and GIS data combined with hourly DAYSIM simulations. Solar Energy, 93 (C), 127-43.

INTRODUCTION

As our knowledge of how to technically make individual buildings more energy efficient matures, the challenges to accomplish widespread adoption of energy saving measures are changing. For individual building owners, implementing energy efficiency measures has become primarily a question of obtaining meaningful information regarding installation costs, potential energy savings and payback times. In tandem with our advances in building technology, cities in many countries now command unprecedented access to data of their jurisdiction's building stock which can be further analyzed and mapped to inform policy decisions. Within this context, it has become increasingly popular for cities and municipalities to create 'solar potential maps' with the intent of promoting renewable energy generation through photovoltaic (PV) panel installations within their jurisdictions. In the United States, larger cities such as Boston, Los Angeles, New York City and Portland provide online maps which allow building owners to look up their address and view personalized predictions such as,

- electric production from a PV system (kWh)
- energy savings from a solar hot water (SHW) system (therms)
- resulting annual electricity savings (dollars)
- carbon savings (lbs)
- useful roof area for installing PV panels (sq. ft.)
- system payback period (years)
- system costs (dollars)
- local rebates and incentive programs (dollars savings)

Table 1 Survey of Existing Solar Potential Mapping Methods in North America

CITY	URL	FLAT ROOF	METHOD (2012)	METHOD (2013)
Anaheim	http://anaheim.solarmap.org/	No	Solar Analyst	Unknown
Berkeley	http://berkeley.solarmap.org/	Yes	Constant	Unknown
Boston	http://gis.cityofboston.gov/SolarBoston/	Yes	Solar Analyst	Solar Analyst
Denver	http://solarmap.drcog.org/	No	Unknown	PVWatts
Los Angeles	http://solarmap.lacounty.gov/	No	Unknown	Unknown
Madison	http://solarmap.cityofmadison.com/madisun/	No	Constant	PVWatts
New York City	http://nycsolarmap.com/	No	Solar Analyst	PVWatts
Portland	http://oregon.cleanenergymap.com/	Yes	Constant	No longer exists
Salt Lake City	http://www.slcgovsolar.com/	No	Solar Analyst	Unknown
San Diego	http://sd.solarmap.org/solar/index.php	?	Unknown	Unknown
San Francisco	http://sf.solarmap.org/	Yes	Constant	Constant
Sacramento	http://smud.solarmap.org/	No	--	Unknown
Orlando	http://gis.ouc.com/solarmap/index.html	No	--	Unknown
Various	http://www.geostellar.com/	No	--	Unknown

The objective of these maps and accompanying personalized property information is to increase the environmental awareness of residents, reduce greenhouse gas emissions and to improve the sustainable image of a city through the expansion of solar energy technology. While a number of cities have already generated such solar maps, to the

authors' knowledge, limited attention has been paid to the assumptions and calculation methods underlying these maps. This paper is organized as follows: Initially a survey is conducted of existing solar potential maps in the United States as well as of existing research. The underlying methodologies used in practice and research are discussed in detail. We then present a new method of how a validated solar radiation calculation algorithm, thus far typically used at the individual building scale, can be combined with an hourly rooftop temperature model and applied to a city-sized model of Cambridge, Massachusetts, USA. The method creates city-wide solar potential maps with a high degree of spatial and predictive accuracy based on the generation of a high resolution three-dimensional (3D) model sourced from available geographic information systems (GIS) data. As a validation of the new method, hourly and daily energy yields from two actual operating PV systems are compared against the new method's predictions using calibrated weather data. Next, results from the new method are compared with those one would obtain using existing methods. Finally, we discuss what relevance varying simulation results may have at both the individual building owner and city-wide policy level using ten sample buildings from the Cambridge building stock.

The authors conducted a review of solar potential maps for North American cities (Table 1). In March of 2012, eleven maps were surveyed, and one year later thirteen maps were surveyed. We found that there are three typical predictive methodologies in place for calculating rooftop irradiation and associated photovoltaic potential. In 2012, three (27%) of the surveyed maps used a constant assumption for solar irradiation reaching a building rooftop, defined in the following paragraph. One (9%) reported using the National Renewable Energy Laboratory's (NREL) PVWatts calculation module (Marion, et al. 2001). Another five (45%) used the Solar Analyst plugin within Esri's ArcGIS program (Fu and Rich 1999). The remaining maps did not report their calculation methodology. In 2013, two maps switched to PVWatts as their prediction method, raising its usage to 23% of available North American solar potential maps. Simultaneously maps reporting using Solar Analyst dropped to just one (7.7%). In reality, the picture this paints is a skewed one. Of the thirteen maps surveyed which still exist, 39% (Anaheim, Denver, Madison, Sacramento and Orlando) require manual input of slope, azimuth and system size. These maps do not automatically map solar potential, but they often have accompanying raster graphics of sunlit hours to help users define their systems.

Outside of already existing solar potential maps, there are several methods which have emerged from research. R.sun (Šúri and Hofierka 2004) has been used to map solar potential for large geographic areas and cities, but it has not, to the author's knowledge, been used in city-scale public solar potential mapping applications such as those detailed in Table 1. PV Analyst (Choi et al. 2011), PV-GIS (Šúri, Huld and Dunlop 2005) and a series of other solar irradiation and photovoltaic calculation methods and case studies are also discussed in the proceeding paragraphs.

Solar potential maps using a constant assumption simply predict that every point on a rooftop receives the same amount of solar irradiation irrespective of orientation and surrounding context. Usually this value is derived from annual global horizontal irradiation measurements from a nearby weather station. Such use of a constant, solar radiation value across a rooftop will be inaccurate in many cases, for example buildings with peaked roofs where each surface of the roof is oriented towards a different section of the sky. The use of a constant value also does not consider local urban context such as trees and neighboring buildings, which shade building rooftops. Those who employ this approach determine the useful roof area for PV installation by using either a constant percentage (Oregon Clean Energy Map 2012) or based on orthophotographic image analysis techniques (San Francisco Solar Map 2012 and Berkeley Solar Map 2012).

The NREL PVWatts web service uses a considerably more detailed method (Marion, et al. 2001) in which hourly solar irradiation is distributed on a 40km square grid for the entire United States based on the typical meteorological year 2 (TMY), dataset (Marion et al. 2001). Local TMY2 irradiation data is used in combination with a manually input DC power rating, PV panel tilt and orientation as well as model-derived panel temperature conditions and climate-based sky models to determine energy production. While roof shape is treated with greater detail than in a solar constant approach, shading and reflections from adjacent urban surfaces also cannot be modeled using PVWatts. This suggests limited applicability in dense urban areas where buildings and trees may shade future PV panels. PVWatts has been validated by Cameron, Boyson and Riley (2008) using measured data from an unshaded, rack-mounted system. It was shown that PVWatts is accurate with an average bias between 9.6 to 10.2%. However, an interface such as PVWatts is difficult to automate for an entire city as every roof surface with a differing slope and azimuth must be input separately. The New York City Solar Map (2013) automates this practice, but all other existing maps using PVWatts do not.

Esri's Solar Analyst plugin represents the city as a digital elevation model (DEM). A DEM is a geolocated raster image where the values of individual pixels correspond to elevation measurements. A sky mask is initially generated based on the surrounding pixel values for each pixel in the DEM. Direct and diffuse components of irradiation are calculated based on the amount of the sky which can be seen from each pixel. Direct irradiation is calculated in accordance with the sun position, the slope of the DEM, a fixed sky transmissivity coefficient, and the distance a solar ray must travel through the atmosphere. Diffuse irradiation is calculated in much the same way as the direct component, based on either a uniform sky model or a standard overcast model; however, no solar map reports on its website which sky model was used. As Solar Analyst uses only a sky mask based on a DEM, it has no capacity to model reflected radiation from neighboring buildings, surrounding trees or the urban terrain. It has been proposed to assume a directional constant of reflected irradiation for obscured sky areas (Rich, et al. 1994), but it would be inadequate to consider complex reflections from surrounding buildings and landscape. In Solar Analyst, sky transmissivity and the ratio between direct and diffuse insolation are fixed, constant values throughout the year. These assumptions can have significant impact on calculated annual irradiation. For example, the Boston Logan TMY3 weather data illustrates a ratio between direct and diffuse irradiation which varies widely throughout the year (US Department of Energy 2012). Figure 1 displays diffuse horizontal irradiation versus direct horizontal irradiation from this data. Points are shaded based on the observed cloud cover at that hour. The mean direct-to-diffuse ratio of insolation for Boston is 64%; however, the standard deviation from the mean is 31%, and neglecting this variance is obviously incorrect. The reader may for example imagine a site with predominantly clear skies in the morning and cloudy afternoons. For that site an east-facing surface receives considerably more solar radiation than its west-facing counterpart, a climate-specific idiosyncrasy that Solar Analyst cannot resolve.

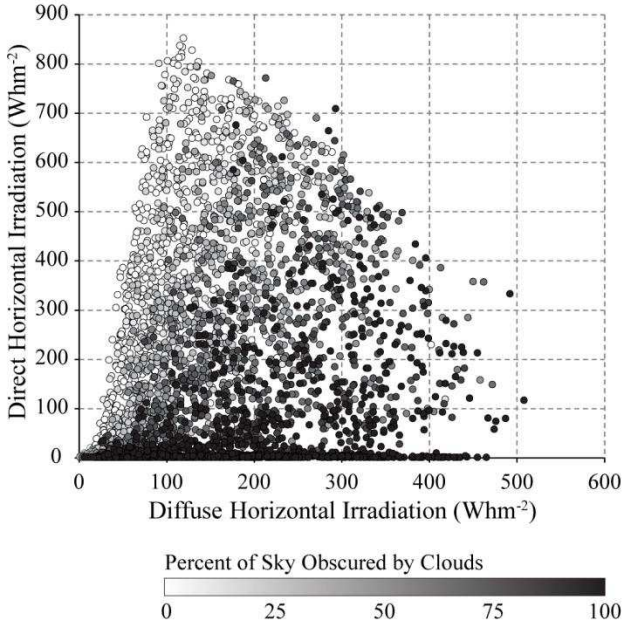

Figure 1 Hourly Direct and Diffuse Radiation and Cloud Cover from Boston Logan TMY3 Weather Data

R.sun (Šúri and Hofierka 2004) is a model implemented in the open source GRASS GIS program (GRASS Development Team 2013) which resolves perceived limitations noted in the Solar Analyst model. One major difference compared to Solar Analyst is that r.sun has the ability to model the solar insolation of very large geographic areas which transcend several differing climate zones by setting the percent of direct and diffuse irradiation as spatially resolved raster images rather than as fixed values as in Solar Analyst. A second notable difference is that r.sun makes a provision for ground reflected solar irradiation; however, its model assumes that all ground reflection is accounted for by surface inclination, global horizontal irradiation and ground albedo which does not account for shaded or unshaded portions of ground nor the actual geometry of its context. While r.sun is deployable across geolocated raster DEMs, it has significant limitations in usability for the purpose of annual city-scale photovoltaic potential maps. The first limitation is that r.sun is only capable of modeling a single day or hour of irradiation at a time. This means that a detailed annual calculation requires at least 365 raster results images to be created and processed independently. A second limitation is that direct and diffuse percentages of irradiation can

only be set as raster image inputs and not as fixed values meaning that for modeling a small geographic area such as a city, it is inconvenient to model climactic effects. To model the typical daily changes from a source such as a weather file, it is necessary to create separate beam and diffuse percentage raster images for every day in the year. To consider typical hourly changes, as in the case of the example above where a city has clear mornings and cloudy afternoons, raster images need to be created for every hour in the year. It is appropriate to mention here than GRASS has a powerful scripting engine which can help in managing this task.

Besides the methods discussed in the preceding paragraphs, many others have documented their process towards analyzing photovoltaic potential in cities and neighborhoods using GIS data and various simulation programs. PV-GIS (Šúri, Huld and Dunlop 2005) is a web-based tool similar to PVWatts supporting African and European analysis which uses calculations from r.sun modified by measured direct and diffuse monthly average irradiation raster images as its underlying weather data source. PV Analyst (Choi et al. 2011) coupled TRNSYS simulations of photovoltaic panels with a DEM in Esri's ArcMap tool, suggesting a desire for the application of validated algorithms in solar potential modeling; however, the tool is yet to be released. PV Analyst relies on Solar Analyst for shading calculations and TRNSYS for irradiation and PV yield calculations. Others (Brito et al. 2011, Nguyen and Pearce 2010, Nguyen and Pearce 2012), have used monthly averaged beam and diffuse solar data with r. sun to calculate photovoltaic potential of relatively small urban developments. Hofierka and Kanuk (2008) perform the same without noting how climate is accounted for. However, r.sun has mostly been applied to very large areas such as Europe and Africa (Šúri, Huld and Dunlop 2005, Bergamasco and Asinari 2011, Huld, Müller, and Gambardella 2012, Ruiz-Arias 2012, Palmas et al. 2012), and its raster-based input methods suggest the tool is most appropriate for large geographic areas. Lukač et al. (2012) calculated direct and diffuse irradiation based on measured climate data, roof slope and aspect and overshadowing potential from neighboring buildings and landscape. Schallenberg-Rodriguez (2013) eschews using a simulation engine at all by suggesting that for regional feasibility studies, relatively simple spreadsheet calculations are adequate; however, for spatially detailed building-rooftop analysis, such calculations are not capable of accounting for shading from contextual geometry or detailed resolutions of roof shape.

Geometric and Material Assumptions

Of the surveyed solar potential maps, four (28.6%) assume that all buildings in the city have flat roofs at a known elevation, four (28.6%) used a detailed DEM, five (35.7%) relied on user input to represent the roof slope and aspect, and the remaining map did not report its assumptions. Of cities utilizing the flat roof assumption, half assumed that a fixed percentage of the roof is suitable for PV (Boston, Portland). The others relied on a proprietary orthophotographic image analysis method for locating rooftop obstructions (Berkeley, San Francisco). Maps using DEMs determine useful roof area either by the predicted rooftop irradiation or by the number of daylit hours observed in a year. The effect on simulation results of assuming a flat roof are discussed later in the paper.

The source height measurements for DEMs often come from LiDAR, Light Detection And Ranging. LiDAR is an established, accurate measurement system wherein a surveying aircraft emits rapid laser bursts and records the time until their visual return while tracking its location via Global Positioning Systems (GPS). The collected location and timed return data is later processed into geographically located point data. Practically, LiDAR is the most accurate way to measure an entire urban area, including detailed roof forms and landscape. The majority of detailed solar potential surveys of urban areas use LiDAR point measurements in constructing digital elevation models to use as input to solar irradiance calculations (Brito et al. 2011, Nguyen and Pearce 2010, Nguyen and Pearce 2012, Yimprayoon and Navvab 2010, Lukač et al. 2012, MadiSUN 2012, Geostellar 2013).

None of the surveyed cities or research methods discussed in this section employ a method which considers physically accurate reflections from urban context.

METHODOLOGY

LiDAR Data, Accuracy, and the Construction of a Detailed Three-Dimensional Model

The authors' implementation of an urban solar potential map is based on the creation of a detailed 3D model in the validated Radiance / Daysim backward-raytracing daylight simulation engine (Ward 1995, Reinhart and Walkenhorst 2001). The advantages of creating an actual 3D representation of the city compared to a DEM are that roof surfaces can be properly modeled as smooth sloping planes rather than a pixelated height representation and

that accurate reverse-raytracing simulations can be implemented that account for reflections and shading from the surrounding context. The geometric information used in creating the 3D model of Cambridge comes from a 2010 LiDAR survey of the city. The vertical accuracy of the data in the urban context of Cambridge was bounded to less than 1m root-mean-square error (RMSE). In validation tests of selected areas the RMSE between LiDAR and traditional GPS measurement methods was shown to be 0.062m (Alliance for Sustainable Energy 2010).

The employed process of creating a detailed 3D urban model is illustrated with an example surrounding the Kresge Oval at the Massachusetts Institute of Technology in Figure 2. As LiDAR data is not uniformly sampled in plan, it creates an awkward data space (Figure 2(b)) where different point densities are present depending on the airplane path of flight. Initially, there were 126,624,764 points spread across Cambridge, which has a total area of approximately 18.5 km^2 (4,500 acres). We uniformly resampled the LiDAR data over a plan grid of approximately 1.25x1.25m (4'x4') spacing, taking the mean of the first return data where multiple points existed. Resulting neighboring points which did not vary by greater than 0.3 meters vertically were discarded. This resulted in a simplification of the data space to a mere 9,403,750 points without losing much geometric resolution. The simplified LiDAR-derived points were then divided into two categories using publicly available GIS datasets from the City of Cambridge: buildings and ground scape (Figure 2(c)) (City of Cambridge 2004). As a final step, the two groups of points were triangulated using a Delaunay algorithm (Figure 2(d)), resulting in a highly accurate and detailed 3D model of the entire City of Cambridge that consists of 16,547,790 triangular surfaces.

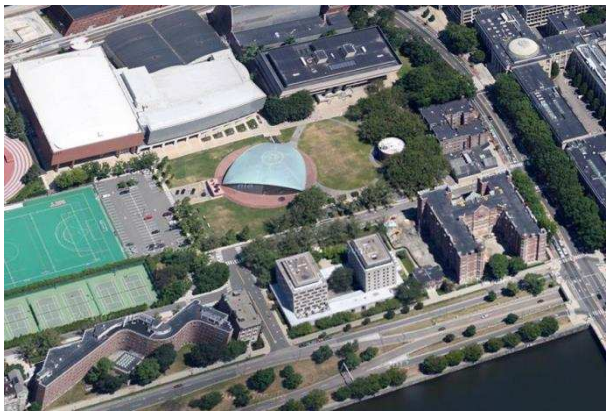

(a) Birds-eye image of the Kresge Oval (Google)

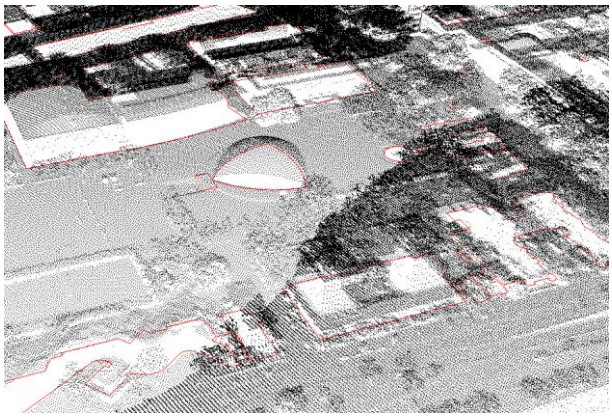

(b) Initial, nonuniformly dense LiDAR point data

(c) Resampled and categorized LiDAR points

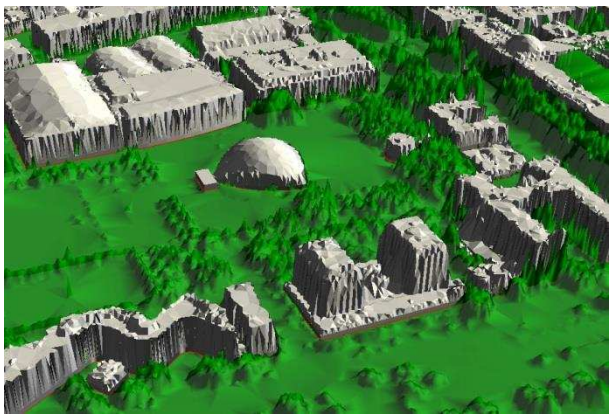

(d) Resulting 3D model

Figure 2 Process Images of 3D Model Generation from LiDAR and GIS Data

Hourly Simulations with Radiance/Daysim

The triangulated surface model was then converted into the Radiance backward raytracer format. In Radiance each surface may have different, highly customized, optical surface properties. In the authors' model it is assumed that building walls are Lambertian diffusers with a 35% reflectance while the surrounding landscape has a diffuse reflectance of 20%. Rooftop reflectances and absorptivities were calibrated based on information from the City of Cambridge Tax Assessor's Database for roofing material (City of Cambridge 2011). Annual irradiation was then calculated on each building roof surface at a grid resolution of 1.5x1.5m (5'x5'). Simulation sensor points are located approximately 0.5mm (1/64") above and facing in the normal direction of the roof surface.

Simulations are performed with Daysim, a validated fork of the Radiance program that uses a daylight coefficient approach (Mardaljevic 2000) and the Perez all-weather sky model (Perez, et al. 1993) to predict annual point illumination and irradiation while considering climate-specific data (Daysim 2013). Daysim works by performing one raytrace operation to a sky dome consisting of 145 diffuse sky segments, 3 ground segments and a second raytracing run with approximately 65 direct solar positions that are distributed along the annual solar path. By tracing backwards from the simulation sensor points, each sky segment and solar position is then weighed relative to its contributions to each point in the scene. In this manner, irradiation can be simulated for an entire year in any incremental time step without running thousands of separate and lengthy raytracing calculations while considering measured typical climate information, contextual shading and reflections based on a detailed three-dimensional geometric model. In the author's study, irradiation simulations were performed at an hourly timestep. Daysim has been shown by many studies to be highly accurate in modeling visible wavelength natural light in diverse climates and sky conditions (Reinhart and Walkenhorst 2001, Reinhart and Andersen 2006, and Reinhart and Breton 2008, Jakubiec and Reinhart 2013). Ibarra and Reinhart (2011) compared Daysim predictions of irradiation against a measured dataset and showed that Daysim is able to accurately resolve temporal variations in longwave solar irradiation in urban contexts.

Table 2 documents the Daysim simulation parameters used in the authors' simulation in order to ensure simulation accuracy. Parameters were primarily considered in relation to the unusually large size of the Cambridge model. Errors in the ambient calculation were calibrated to be acceptable for surfaces spaced four feet apart and larger. As the model was resampled at this resolution in plan and simulation sensor points are spaced beyond this threshold, the assumption seems reasonable. According to Ward, error will "increase on surfaces spaced closer than the scene size divided by the ambient resolution" (Rtrace man page 2012). Thus the Radiance scene size of 26,526.5 ft divided by four gives an ambient resolution of approximately 6,750. This means that ambient interpolation is unlikely to occur across separate triangles in the scene which may have different orientations and solar condtions. Ambient divisions are set at 2048 such that for each sensor point and ray reflection, 2048 rays are cast to sample the ambient environmental conditions. In essence, the model accounts for any geometry which occupies a perceived solid angle larger than 0.0031 sr. Direct contribution is sampled deterministically for each ray reflection. The simulation considers up to two ambient reflections from direct solar irradiation and one reflection from diffuse sky irradiation from the environment (ambient bounces, ab).

Table 2 Key Radiance/DAYSIM Simulation Parameters

PARAMETER	DESCRIPTION	VALUE
ab	ambient bounces	2
ad	ambient divisions	2048
as	ambient super-samples	16
ar	ambient resolution	6750
aa	ambient accuracy	0.1

Calculation of Photovoltaic Yield

As previously discussed, a key benefit of the new method is direct access to hourly simulated irradiation data and the detailed Perez sky model that approximates actual sky radiance distributions for each hourly time step in the year. Knowing in addition the explicit area beneath each simulated point and information about the urban climate, a reasonable calculation can be made for the performance of a PV panel in an urban context.

A direction vector is assigned to each simulation sensor point based on the normal direction of the roof surface immediately below it. Assuming that the roof is planar and unvarying below the area the point represents, ~1.5m^2 in this case, a method of calculating the area is shown in Equation 1 and illustrated in Figure 3, where $\vec{n}$ is the unitized roof surface normal vector.

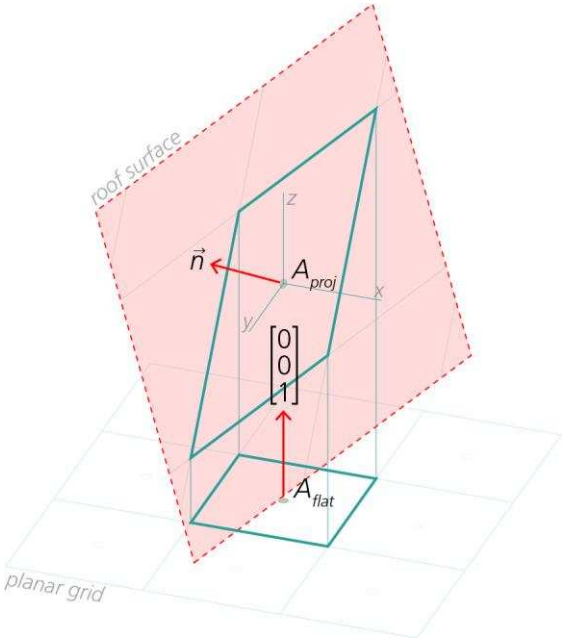

Figure 3 Illustration of the geometric terms in Equation 1

$$A_{proj} = \frac{A_{flat}}{[0 \quad 0 \quad 1] \cdot \vec{n}} \tag{1}$$

$$T_{sol-air} = T_{amb-air} + \frac{(\propto * E)}{h_c} \tag{2}$$

$$T_C = T_{sol-air} + \frac{(T_0 - 20°C) * E}{800 W m^{-2}} \tag{3}$$

$$P_{mp} = P_{mp0} * \ [1 + \gamma * (T_C - T_0)] \tag{4}$$

PV performance is dependant on many factors which are unknown at the time of making a conceptual irradiation map such as module efficiency, panel orientation, wiring and equipment and maintainance conditions. However, it is known that high ambient temperature and solar radiation heating up the panel will have an adverse effect on its production. Furthermore, air temperatures near urban rooftops will be higher than the ambient air temperature due to the effects of solar radiation; therefore, the sol-air temperature is used to approximate this phenomenon, shown in Equation 2. The sol-air temperature is the urban ambient temperature ($T_{amb\text{-}air,}\ °C$) plus the absorptivity of the roof ($\propto$, percent) multiplied by the incident irradiation (E, Wm^{-2}) and divided by a convective and radiative loss factor (h_c, Wm^{-2}-K) which we assume to be a constant 15 Wm^{-2}-K. In the model, rooftop absorptivity is estimated per building based on roof type data in the Cambridge Tax Assessor's database (City of Cambridge 2011). The sol-air temperature is used to predict panel temperatures in Equation 3 by relying upon knowledge of the nominal operating cell temperature at Nominal Operating Cell Temperature (T_0) (Luque and Hegedus 2011). Further, the photovoltaic maximum power at ideal conditions (P_{mp0}, W) can be derated based on a temperature correction factor (γ, %/˚K) (Equation 4) (Marion, et al. 2001). The temperature correction factor is usually provided by PV panel manufacturers with panel specification information. Huld et al. (2006) predicted monthly average temperature profiles of Europe to use in calculating PV efficiency reductions. Their results were implemented in the PV-GIS web service; however, an annual efficiency reduction factor was used. In the authors' new method, it is possible to resolve this efficiency loss on an hourly basis.

Equations 1-4 are used as a first-order approximation in derating panel efficiency based on ambient air temperature and point irradiation at each hourly timestep.

Determination of Useful Rooftop Area

Useful rooftop area in the model is calculated based on the predicted economic feasibility of panels installed at a location. Any roof surface sloping greater than 60 degrees (67%) was discarded and instead considered to be a vertical surface or wall. The reader should note that this cutoff was an arbitrary choice and the method itself would also be capable of modelling façade integrated photovoltaics by generating simulation sensors on such wall surfaces.

No rooftop setback was considered in this study; therefore, useful rooftop area can extend to the edge of the roof surface.

According to the Massachusetts Clean Energy Center, in 2011 the average PV installation costs were $5.67 per watt in Cambridge (MassCEC, 2012). Assuming a typical panel that is rated at 185W/m^2 (17.2 W/ft^2) (Sunpower E18/230W 2012), the installation cost follows to be \$1049.70/m^2 (\$97.52/ft^2). The 2012 Cambridge cost of electricity for residential customers was $0.15/kWh which is fixed for the duration of the financial analysis. Requiring a ten year investment period with a ten percent discount rate per year, 1244.9 kWh/m^2-yr (115.7 kWh/ft^2-yr) would have to be generated to have a net present value (NPV) in which the investment breaks even, when NPV equals zero. An ideally oriented solar panel in Cambridge receives approximately 1600 kWh/m^2-yr (149 kWh/ft^2-yr) of solar irradiation annually and would hence require a panel efficiency of nearly 80% in Cambridge for the system to break even in ten years. If one only required a simple payback over the same 10 year period, the panel efficiency would still need to be nearly 50%.

National and state rebate programs that exist to improve the economic feasibility of PV for residential properties seriously change the financial outlook of such installations. In 2012 the US federal government offered a 30% tax rebate on the cost of a PV installation (Energy Improvement and Extension Act 2008). Further, Massachusetts offered a 15% rebate up to a maximum of $1,000 that could be carried over for three years (Residential Renewable Energy Income Tax Credit 1979). The Massachusetts Clean Energy Center offered a minimum $0.40/W rebate on new PV systems (MassCEC 2012). Massachusetts also offered a 100% protection from increased property taxes due to PV installations for a 20 year period (Renewable Energy Property Tax Exemption 1975). Finally, Solar Renewable Energy Certificates (SRECs) are ways of trading proof of generating sustainable energy as a commodity. The 'floor'price of these commodities is currently valued at $0.285/kWh (DSIRESOLAR 2012). Factoring these rebates and incentives into the previous NPV calculation, it is possible to have a break even point for an unshaded panel at 7.5% efficiency without accounting for future energy prices or PV panel degredation. This means that considering an investment period of 10 years for an example Sunpower panel, any point which has the capacity to generate over 121 kWh/m^2 (11.25 kWh/ft^2) of energy per year is likely to recoup its value while providing additional savings after the initial 10 year period as the effective lifetime of a PV system is known to be typically greater than 30 years. Thus such points and their associated roof areas are considered to be useful to install PV panels. As the point-based simulation results from this study are displayed spatially (see results section), it is possible to determine optimal placement locations for PV panels coincident with urban rooftops.

Geolocation of Data From GIS to Radiance Simulation Models

All GIS models including the LiDAR data and building footprints were constructed in the projected North American Datum 1983, Massachusetts State Plane Mainland coordinates system (Schwarz and Wade 1990). This is a serendipitous choice as distances and areas can still be measured without necessitating geographic corrections. Thus, the Radiance/Daysim simulation model was built in an identical coordinate system. The Massachusetts State Plane system also has a known relationship between X and Y coordinates and latitude and longitude global coordinates. It is possible to translate easily between the two coordinate systems by use of an Inverse Lambert Conformal Conic Projection with proper geospatial parameters.

RESULTS AND DISCUSSION

Comparison of Predictions and Measured Data

The new method was validated against measured energy production from two installed photovoltaic systems in Cambridge. One system is located on the MIT campus' student center building, and the other on a private residence. For each system, hourly measured energy production is compared to hourly predicted energy production. The reader should note that this hourly comparison is only conducted with the new method since most previous methods cannot predict hourly electricity yields and cannot be reasonably calibrated to use custom hourly weather data.

The first of the two systems is a 7.2 kW system installed on the roof of the student center, and the second is a 5.9 kW system in a dense residential area of Cambridge. The student center system consists of 24 Schott 300W panels that were installed approximately nine years ago. The residential system consists of 30 Sanyo 195W panels that are two years old. Detailed information for both systems is contained in Table 3 below, and Figure 4 shows the simulation models used in the validation. Both of the models include the detailed surrounding urban context and

accurate representations of the photovoltaic panels being compared to. The student center system is installed nearly flat with a panel tilt of 5 degrees while the residential system is installed on a peaked roof which has a tilt of 50 degrees. The student center system is primarily unshaded by its context; however, trees and a chimney shade small portions of the residential system during some times of the year near sunset. Furthermore, the student center system has a black asphalt roof while its residential counterpart has a light colored roof. The values reported in Table 3 for rooftop absorptivity were estimated based on visual observations. Because the two models are very different in terms of orientation, geometry and roof color, we suggest that they constitute a reasonable sample of common urban conditions against which to test the new method.

Table 3 System Parameters of Selected PV System

PARAMETER	STUDENT CENTER	RESIDENCE
Panel Count	24	30
PV Model	Schott ASE-300-DGF/50	Sanyo HIP-195BA19
Efficiency at Ideal Conditions	12.3 %	16.8%
Power at 1,000 W/m^2, 25ºC (P_{mp0})	300 W	195 W
Temperature Correction Factor (γ)	0.47 % / ºK	0.348% / ºK
Panel Tilt	5 degrees	50 degrees
Panel Azimuth	22 degrees East of South	3 degrees West of South
Inverter Efficiency	94 %	96%
Panel Age	9 years	2 years
Estimated Rooftop Absorptivity	0.9	0.35

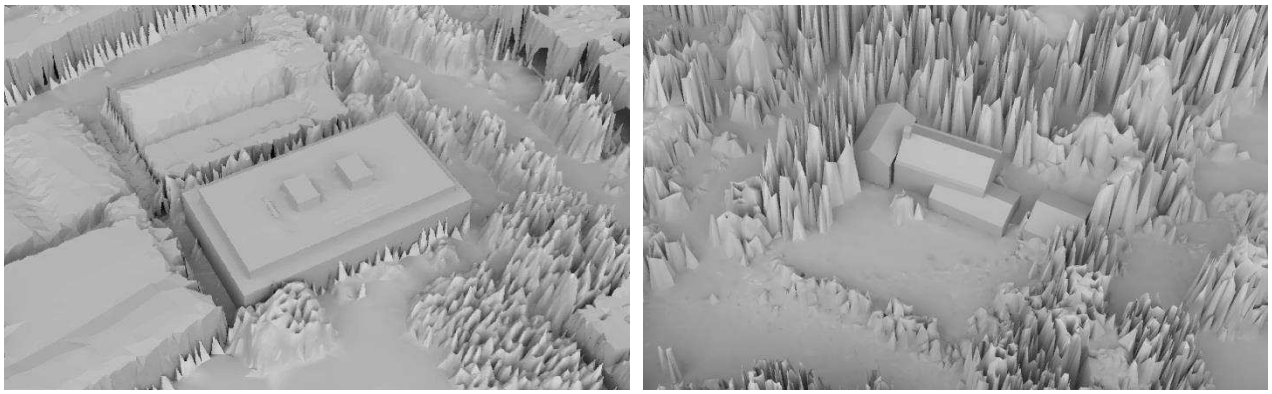

(a) Student Center Simulation Model (b) Residence Simulation Model

Figure 4 Detailed Building Simulation Models in Urban Context

Validation Procedure

In order to compare measured PV energy yields to simulated predictions, it was necessary to use weather data from the period of measurement. For this purpose, global horizontal solar irradiation and ambient air temperature measurements at 15 minute intervals were acquired from a weather station approximately 0.6 miles (1km) away from the MIT campus for the period of July 2011 – June 2012 (Cambridge, Massachusetts Weather 2012). These were averaged into hourly values, and the resulting global horizontal solar irradiation was converted into direct normal and diffuse horizontal components using the Reindl model (Reindl et al. 1990). Further, the known information in Table 3 regarding the two PV panel systems was employed in calculating the resulting energy production using the same procedure as explained in the methodology section. Panel efficiency was further reduced by a factor of 0.5% per year of operation as has been shown typical in the studies of King and Quintana (King et al. 1998, Quintana et al. 2002). For example, the nine year old student center PV system is reduced by a factor of 4.5% as it is nine years old such that the calculation $12.3\% * (1.0 - 9yrs * 0.005\%/yr)$ results in a reduced base efficiency of 11.75%. Detailed geometric models of the panel systems were digitally constructed to remove geometric differences as factors in the comparison.

Typical Summer and Winter Week Hourly Simulation Results

Figure 5 illustrates typical summer and winter weeks of hourly measured and simulated data for both analyzed PV installations. The residential system does not have winter week information as there was systematic missing and shifted data for that portion of the year. The solid black lines represent measured energy generation while the red lines indicate predicted energy generation by our model using the predicted sol-air temperature. The black dotted lines show predicted energy generation using the ambient urban air temperature. Figures 5(a) and 5(b) show results for the student center system. 5(a) illustrates a summer week in 2012. For this week, measured and predicted energy values are very similar with a RMSE which is 4.4% of the rated system capacity during daylit hours. 5(b) shows similar results during the 2011 winter with a RMSE equating to 4.7% of the system capacity during daylit hours. 5(c) illustrates a typical summer week of the residential PV system. Its RMSE during daylit hours is 7.3% of the rated system capacity. Overall, the good agreement between simulation results and measured data suggests that the new method is capable of accurately representing temporal changes in PV yield during hot and cold periods of the year.

An interesting observation is that the effect of high rooftop temperatures is very strong during hot Summer days in Cambridge, especially for the unshaded student center system located on the dark roof with an estimated absorptivity of 0.9. Figure 5(a) shows that the predicted energy using ambient temperature (black dotted line) varies from the measured and predicted energy values (solid black and red lines) for the student center by on average 18.3% during the summer week. The maximum deviation during this same time is 36.7% on 7/3. Figure 5(c), displaying the residential system's PV yields, reports a weaker temperature effect because its panels are less sensitive to changes in temperature (see temperature correction factor (γ) in Table 3), and the rooftop of the residential system is clad in a lighter colored material having an estimated absorptivity of 0.35. During the winter, the ambient temperature is cold enough that it is a rare occurrence where the predicted energy using ambient air temperature and sol-air temperature vary; however, on 12/16 and 12/20 shown in Figure 5(b), there are peak periods where there is an observable reduction in predicted energy generation due to higher PV panel temperatures. These observations suggest that the consideration of urban rooftop temperature is important in understanding photovoltaic yields of panels coincident with rooftops, especially in climates that are warm for a portion of the year and for buildings with highly absorptive roof surfaces.

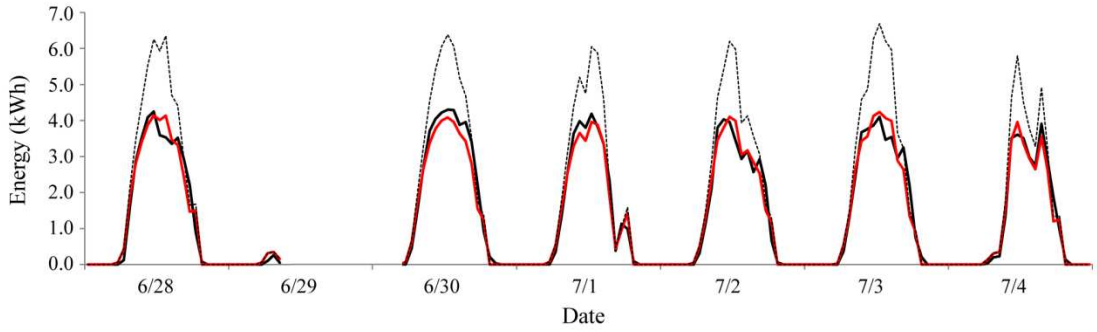

(a) Student Center Measured vs Simulated Summer Week Hourly PV Energy Production

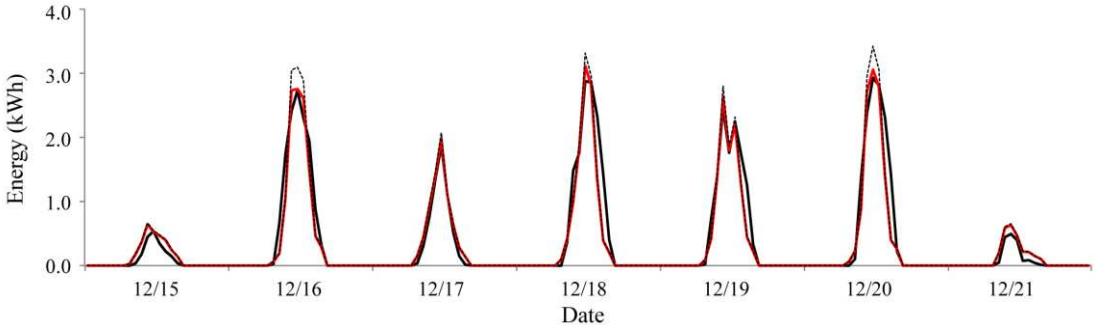

(b) Student Center Measured vs Simulated Winter Week Hourly PV Energy Production

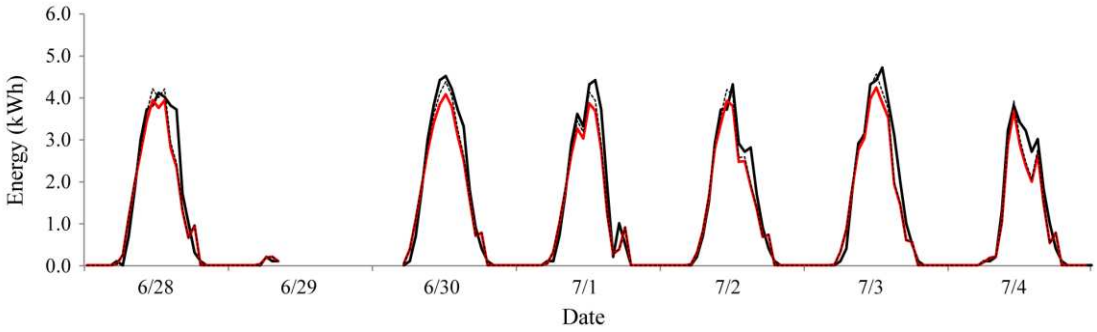

(c) Residence Measured vs Simulated Summer Week Hourly PV Energy Production

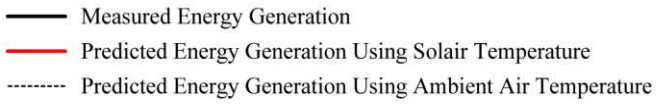

Figure 5 Hourly Results of Simulations Compared to Measurements for Example Winter and Summer Weeks

Daily Results

Cumulative daily energy production information was available for each system. Figure 6 contains daily information from the second half of 2011 and the first half of 2012; therefore, it constitutes an entire year of analysis. Days where measured weather data was not available or there were errors in the measured PV yield datasets were removed from this analysis. The plots 6(a) and 6(b) show measured energy production on the horizontal axis and predictions of energy production on the vertical axis. The identity lines on each illustrate an ideal data distribution where prediction matches reality perfectly. It can be seen that for all simulated days the agreement between simulations and reality is strong as points are clustered about the identity lines. For the student center PV system, the daily RMSE is 9.3% of the daily average production of 21.72 kWh. The RMSE of the residential system predictions is 9.4% of the daily average production of 23.22 kWh. The greatest error is observed on partially cloudy days where the Perez sky model is unable to resolve the position of clouds in the sky based solely on measured global horizontal irradiation.

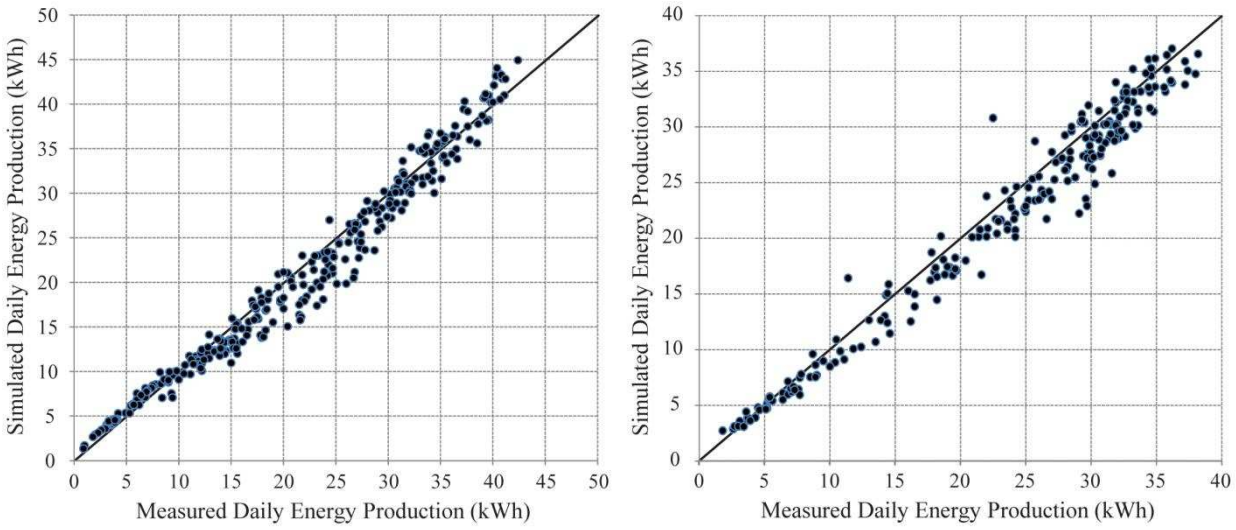

(a) Student Center (b) Residence

Figure 6 Measured vs Simulated Daily PV Energy Production

Annual Results

Annually the student center simulations predicted 3.6% less energy production than was measured (6365.7 kWh measured, 6136.5 kWh simulated). The residential system predicted 5.3% less energy production than was measured (5154.6 kWh measured, 4881.3 kWh simulated). To help contextualize the meaning of these numbers, predictions were made for each system using a complete set of measured irradiation and temperature data from the same weather station for 2008, 2009, 2010 and 2011. The maximum variance in predicted production between the four years was 5.19% and 5.82% for the student center and residential PV systems respectively. This suggests that the predicted annual error using the new method presented in this paper and calibrated weather data is less than variance which can be expected from climactic differences between years.

Methodological Comparison – Two Cambridge Rooftops

In the previous section it was demonstrated that the new method is accurate within 3.6 to 5.3 percent annually when compared to measured data and calibrating for actual weather. Since the prediction methods reviewed in the introduction cannot accommodate measured weather data as input, this section compares simulation results from the new method for the two Cambridge rooftop systems to the calculation methodologies reviewed in the introduction. The methods used in the comparison are PVWatts, Solar Analyst, r.sun and a solar constant methodology. In all cases, the closest possible geometric models were used. Using PVWatts, the exact geometric parameters of each PV array were input into the program. For Esri's Solar Analyst and r.sun, a highly detailed DEM was created based on a point sampling of the geometric models pictured in Figure 4 every 0.125 meters. Furthermore, we assume that all

methods have perfect knowledge as to the area of the installed PV panels; however, for the solar constant method and any which assume that a building's roof is flat, this assumption is not actually true. As documented in Table 3, the student center PV array is nearly flat, with a panel tilt of 5 degrees. On the other hand, the residential PV array is tilted at a 50 degree angle; therefore, comparisons using flat roof assumptions were added for the residential system in order to illustrate the importance of geometry in city-scale PV potential modeling. **.** The flat roof calculations use perfectly flat roofs which do not accurately represent actual rooftop geometry; however, they do include urban context. Our new method uses typical meteorological data (United States Department of Energy 2012) for this comparison as discussed in the methodology section. The Solar Analyst calculations herein use the Esri-defined default ratio between direct and diffuse radiation. As is common in the earlier reviewed literature, r.sun calculations use a standard Linke turbidity factor for urban environments which varies monthly (Hofierka, Šúri and Huld 2013). Raster image representations of beam and diffuse clear sky index (Šúri and Hofierka 2004) were created by comparing monthly averages of global horizontal beam and diffuse clear sky radiation calculated by r.sun with average measured values from the Boston weather file (US Department of Energy 2012). These raster images were used as inputs to r.sun in order to account for realistic sky conditions. The values of clear sky index must be between zero and one. For Cambridge, computed beam clear sky indices for r.sun ranged between 0.47 to 0.57; however, computed diffuse clear sky indices ranged between 1.29 to 1.72. These values greater than one are forced to one which results in r.sun underestimating the diffuse component of radiation present in Cambridge.

Figure 7 illustrates monthly comparisons of the predicted energy yields using the various calculation methodologies described previously. 7(a) shows results for the student center PV system, and 7(b) shows results for the residential PV system. The red line indicates the calculations of our new model, and the pink padding around that line illustrates the monthly RMSE of each system when they were compared to measured data in the previous section. For the student center and residential systems, the monthly RMSEs compared to measured data are 7.25 and 5.65 percent respectively. Table 4 presents annual PV electrical yields, monthly mean bias deviation (MBD), monthly root-mean-square deviation (RMSD), and unbiased monthly RMSD for each existing methodology compared to the new method. Monthly unbiased RMSD accounts for the mean monthly error by forcing the MBD to be zero.

Because the new method has been validated specifically for these two geometric contexts and PV systems, the best performing models from research and practice will approximate the solid red lines which represent the new method in Figure 7. PVWatts (blue line), which has been validated against measured data (Cameron, Boyson, and Riley 2008), produces results very close to those of the new method for both systems. The notable exception to this is that PVWatts calculates greater summer PV yield for the student center system (Figure 7(a)), which suggests that the PVWatts algorithms do not account for the potential excess heating of PV panels when they are installed on dark urban rooftops. This assertion is corroborated by the close agreement between PVWatts and the new method for the residential system (Figure 7(b)), which has a lightly colored roof and PV panels that are less affected by temperature (Table 3). As explored earlier, PVWatts does not have the capacity to account for urban surroundings, so it performs well when modeling systems without many obstructions as in these two examples, but it would not be able to accurately model rooftop systems which are shaded by nearby trees or buildings or advise against such systems in an urban PV potential modeling exercise. R.sun (purple line) also closely follows the predictions of the new model in the nearly flat-roofed context of the student center system. Most existing methods (besides the solar constant and Solar Analyst) predict greater summertime yields for the student center system, likely because they do not account for high enough summer rooftop temperatures. The results obtained by using Solar Analyst (green line) predict far less electrical yield than other models for both PV systems during the winter, resulting in MBD values between -6.2 and -25.0 percent. For the residential system with its sloped roof, r.sun predicts less energy production in the summer than during the winter and results in a nearly constant monthly energy rate. It therefore under-predicts the PV potential of the sloped roof with a MBD of -22.9%. Ruiz-Arias et al. (2009) validated r.sun against measured estimates of global horizontal irradiation which agrees with results shown in Figure 7(a); however, r.sun seems to predict significantly less irradiation than other models under certain sloped-roof conditions. The flat roof methods (dashed lines) applied to the residential system (Figure 7(b)) correlate as a group by having similar monthly energy yields with the exception of Solar Analyst which again predicts significantly less yield during the winter. As the solar constant (grey line) method does not have any built-in mechanisms to track climactic trends, it performs the worst in the case of a flat roof system with a RMSD of 34.3 percent, and it performs artificially well in the case the peaked residential roof which has a more uniform yield profile throughout the year.

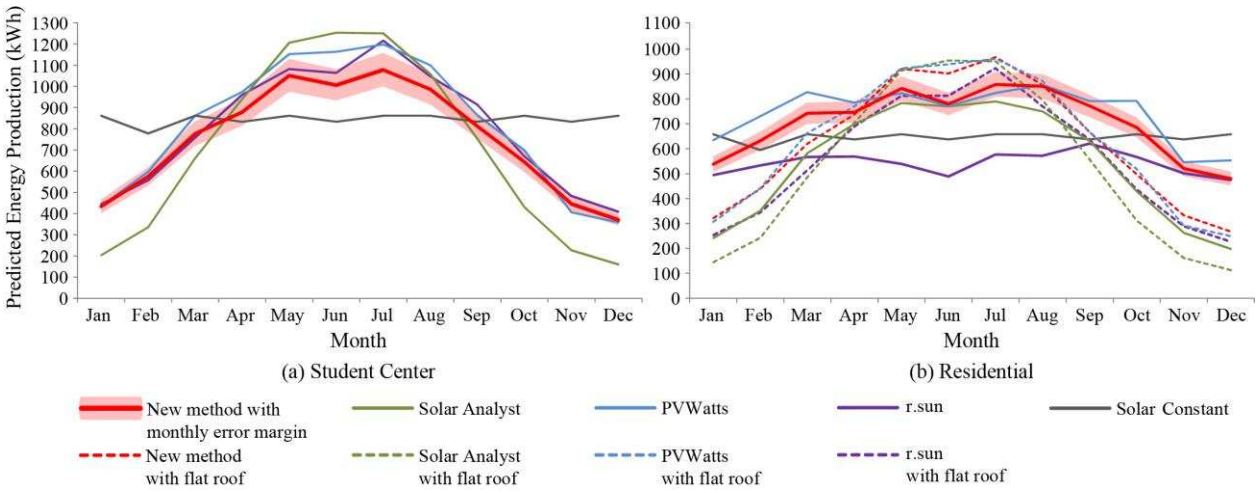

Figure 7 Monthly Comparison of Typical Energy Prediction Methods

Table 4 Typical Annual Results and Percent Errors Compared to Detailed DAYSIM Method

CALCULATION MODEL	ANNUAL PV YIELD (kWh)	MONTHLY MBD (%)	MONTHLY RMSD (%)	UNBIASED RMSD (%)
Student Center PV System				
New method	9,041	--	--	--
PVWatts	9,806	8.5	11.4	7.6
Solar Analyst	8,477	-6.2	23.9	23.0
r.sun	9,571	5.9	8.4	6.0
Solar Constant	10,140	12.2	34.3	32.1
Residential PV System				
New method	8,447	--	--	--
New Method (Flat Roof)	7,527	-10.9	20.9	17.8
PVWatts	8,932	5.7	8.9	6.8
PVWatts (Flat Roof)	7,601	-10.0	21.9	19.4
Solar Analyst	6,486	-23.2	27.4	14.5
Solar Analyst (Flat Roof)	6,334	-25.0	38.3	29.0
r.sun	6,511	-22.9	24.4	14.8
r.sun (Flat Roof)	6,717	-20.5	26.6	17.0
Solar Constant	7,752	-8.2	19.7	17.9

Methodological Comparison – Urban Context

The previous section compared different PV yield prediction methods for two Cambridge rooftop systems. In order to provide the reader with a more comprehensive feeling as to what these differences mean for a city-wide PV potential map, the analysis is expanded to ten randomly selected buildings, which represent the overall building stock of Cambridge. Of these ten buildings, five can be described as having flat roofs; however, they often have HVAC equipment and other obstructions present on the roof such that they are not truly flat. The other five have roofs of some complexity with at least one ridge line. These test buildings are shown in Figure 8. The new method is compared to the existing Solar Analyst, r.sun, flat roof and constant value methods. PVWatts is not included in this section because it is a web-service relying upon manual user input. As the Solar Analyst, r.sun and constant value

methods cannot account for rooftop temperatures or hourly data, a simple 18.5% panel efficiency is assumed for all energy yield calculations in this comparison.

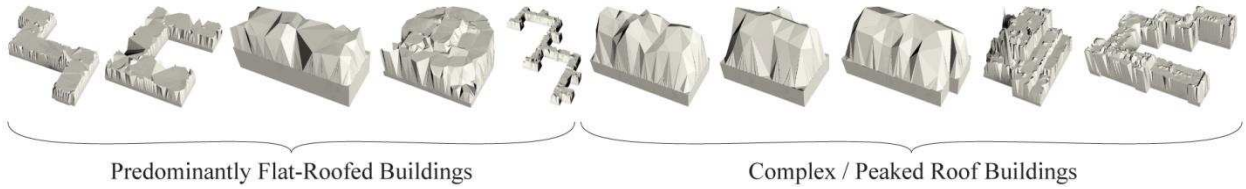

Figure 8 Ten Test Buildings Used in Comparing Results

Table 5 compares annual irradiation predictions using existing methods to the Daysim-based new method. Mean irradiation across all points, MBD and RMSD are reported in total and for each geometric type of rooftop identified in Figure 8. In Cambridge, an unobstructed flat roof receives approximately 1394 kWh/m^2-yr of solar irradiation (United States Department of Energy 2012); however, as noted previously, even 'flat-roofed' buildings are not without obstructions. It is reasonable to wonder how irradiation calculations vary between the methods and common assumptions documented in this paper. The flat roof assumption has a positive bias of 26.2% (MBD) when compared to irradiation calculations which consider actual rooftop geometry. The solar constant method has an even larger bias of 30.3% because it does not account for the urban shading context. These numbers alone suggest that proper representation of geometry is extremely important even in simple solar irradiation calculations, and any rooftop PV potential mapping effort which assumes that all buildings in the city are flat will have obvious inaccuracies. Compared to Daysim's calculations, Solar Analyst and r.sun underestimate annual irradiation with -7.8% and -12.7% MBD respectively. One possible reason for this is that Solar Analyst neglects the reflected component of irradiation (Fu and Rich 1999). On the other hand, r.sun is likely to have an inflated reflected component because it is based solely on view factor, global horizontal irradiation and ground albedo and does not account for shaded portions of the urban context (Šúri and Hofierka 2004); however, as noted previously its model neglects significant percentages of diffuse irradiation.

The large RMSD of the comparison suggests that effects other than calculation bias are at work, and this can be explained by the geometric quality of the simulation models at building edges. Figure 9 shows aerial photographs and planar projections of the predicted irradiation for a single building using different methods which is typical across the ten test buildings. In the process of creating a 3D model of a city, we use building polyline information from GIS databases to create extra points which improve the model resolution at the edge of buildings. As Solar Analyst and r.sun work across a pure DEM which does not differentiate between building and ground, the calculated slope at edge pixels is often extreme and can lead to errors as seen in the upper edge pixels in Figure 9 (Solar Analyst). Such errors will increase as the ratio of building perimeter to plan area increases; however, this effect may be mitigated by considering building-code mandates of roof edge offsets for PV systems that are not included in this study.

Table 5 Predicted Irradiation MBD and RMSD Compared to Daysim-based Calculations

Method	**Mean Irrad.** (kWh/m^2)	**Mean Irrad. Flat** (kWh/m^2)	**Mean Irrad Complex** (kWh/m^2)	**MBD Total** (%)	**MBD Flat** (%)	**MBD Complex** (%)	**RMSD Total** (%)	**RMSD Flat** (%)	**RMSD Complex** (%)
Daysim	1070.0	1130.0	942.2	--	--	--	--	--	--
Solar Analyst	986.6	1049.0	853.5	-7.8	-7.2	-9.4	31.7	32.4	29.1
r.sun	934.0	987.6	820.0	-12.7	-12.6	-13.0	36.3	35.2	38.7
Flat roof	1350.1	1362.0	1324.0	26.2	20.6	40.5	45.8	40.4	58.8
Constant	1394.0	1394.0	1394.0	30.3	23.4	48.0	49.7	43.2	65.3

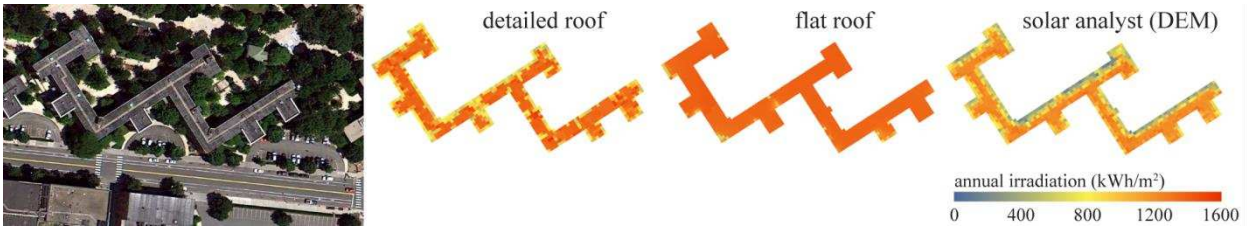

Figure 9 Resulting Point Irradiation Maps For Varying Calculation Methods

It is useful to further qualify this data into PV electrical yields. A simplified equation of annual irradiation (kWh/m^2-yr) multiplied by panel efficiency (18.5%) and area (m^2) is used to calculate the potential electrical yield for this section. It therefore constitutes a way to compare the ability of different models to provide decision-making support when considering installing new PV installations. Keeping with earlier conventions, methods using flat roof assumptions are computed against actual roof areas, although in practice this would not be the case. Using the new method, a PV yield of 2,539 MWh/yr was predicted across all rooftops with a combined 10,949 m^2 of useful roof area. Comparatively, the Solar Analyst method predicted 2,301MWh/yr across 11,041 m^2 of useful roof area, and r.sun predicted 2,183 MWH/yr with 11,967 m^2 of useful roof area. Methods which cannot represent geometry (flat roof, constant value) predict that nearly all rooftop area is acceptable for PV installation and have similar increases in predicted installation cost. This is documented in Table 6 below which displays total PV production determined to be economically useful, the related installation area and predicted installation costs. For this study and for these ten buildings, flat roof assumptions lead to an inability to differentiate between suitable and unsuitable areas for potential PV installations. The r.sun method, while predicting less overall PV production, also concluded that more rooftop areas are useful for PV installations. If such predictions lead to actual PV installations, this would result in installation cost increases between 9 and 22 percent compared to the new method. In reality these increases would be even larger with the hourly rooftop temperature calculations further reducing PV yield predictions of the new method.

Table 6 Simple Annual PV Production, Roof Area and Installation Costs

Method	**PV Production** (MWh/yr)	**Useful Roof Area** (m^2)	**Installed Cost** (millions USD)
New method	2,539	10,949	11.49
Solar Analyst	2,301	11,041	11.59
r.sun	2,183	11,967	12.56
Flat roof	3,323	13,279	13.94
Constant value	3,439	13,336	14.00

To underscore the importance of rooftop geometric accuracy, Figure 10 shows an irradiation map of an urban area in Cambridge with detailed roofs and with assumed flat roofs; each image displays detailed irradiation calculations of the area using the cumulative sky method (Robinson and Stone 2004). The cumulative sky method uses the Radiance reverse raytracer, but under a sky dome which accounts for the solar radiation of every hour in the year. Such a result therefore represents the overall radiation on a surface accounting for geometry, shading and reflections; however, it is not able to resolve hourly temporal information. From Figure 10, it is clearly visible that a flat roof assumption is going to create extreme differences in the results. This is because roof slope will change the angle of incident radiation as well as the percent and portion of visible sky. Overall, the flat roof assumption overestimates available radiation as there are no roof surfaces that slope to the north, nor are there any surfaces that face surrounding buildings; all surfaces are oriented upwards towards the open sky above the building. Further, it is impossible for HVAC equipment or roof projections to shade another portion of the roof. The effects of roof orientation in the ten test cases are higher than the effects of inter-building shading for a city of predominantly low-rise buildings such as Cambridge.

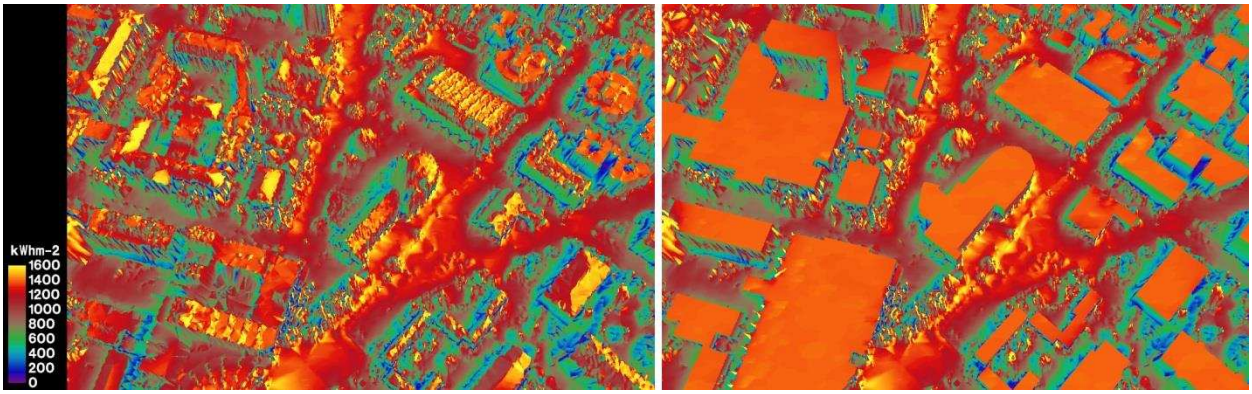

(a) City with Detailed Roof Models (b) City with Flat Roofs

Figure 10 Annual Irradiation Maps (Cumulative Sky Method) for Varying Degrees of Geometric Accuracy

The new climate-based method of calculating photovoltaic potential constitutes the first time that city-level GIS datasets and geometric LiDAR information have been linked to a state of the art, validated daylight simulation tool capable of modeling the effects of shading, reflections and climate-based hourly effects. Such an approach offers exciting opportunities which point towards a new generation of sustainable urban analysis where detailed GIS databases are translated into equally detailed environmental analyses. The results from such analyses can then be fed directly back into the GIS models or a display framework to serve as design feedback for policy and decision makers as well as property owners. As a further proof of concept, the authors partnered with Modern Development Studio, a Boston based architecture and design firm and the City of Cambridge to display results on top of a searchable map document using the Google Maps API, a screenshot of which is shown in Figure 11. The online version of the Cambridge Solar Map is available via http://www.cambridgema.gov/solar/. The map displays the calculated information spatially to map users across their rooftop. Users are also presented with fiscal information in terms of economic impacts, NPV, simple payback periods and local rebate incentives. In this way, building owners and curious users can engage with the map through the ability to identify their roof specifically and notice how its unique form produces varied suitability for photovoltaic installations. Users of the map therefore feel like the simulation results are personalized to their building. The authors believe this is important to produce confidence in the results and to increase interest in the goals of the map.

Figure 11 Public Rooftop Photovoltaic Potential Map of Cambridge, MA (First Version)

To communicate photovoltaic potential effectively, it is necessary to provide useful visual output that aids in the understanding of the data. The simulated rooftop solar potential for Cambridge was accordingly divided into four bins meant to rank the relative predicted performance of a PV panel installed at that point. The thresholds are based on the previously calculated 121 kWh/m^2 (11.25 kWh/ft^2) energy yield for a ten year NPV payback and were calculated such that 15% of the roof area of the city is considered to be 'Excellent.' The four bins are defined as follows,

- N/A < 121.0 kWh/m^2-yr (11.3 kWh/ft^2-yr)
- 121.0 (11.3 kWh/ft^2-yr) ≤ Poor < 165.0 kWh/m^2-yr (15.3 kWh/ft^2-yr)
- 165.0 (15.3 kWh/ft^2-yr) ≤ Good < 219.0 kWh/m^2-yr (20.4 kWh/ft^2-yr)
- 219.0 kWh/m^2-yr (20.4 kWh/ft^2-yr) ≤ Excellent

Admittedly, the detailed climate-based method takes more time and processing power to achieve when compared to generating a model using the flat roof assumption, PVWatts, Solar Analyst or r.sun. For this study, each building in the city took approximately three hours of simulation time using one comprehensive model of Cambridge. This model was approximately eighteen square kilometers (7 mi^2) and contained 16,547,790 triangular surfaces. Later studies tested tiling the model in one kilometer grid cells. With this reduced model size of approximately one million triangular surfaces per grid, buildings took five minutes on average to simulate. The simulations can also be run fully in parallel to increase calculation speed. The solar constant method is instantaneous, and PVWatts relies upon external processing power. Esri's Solar Analyst tool and r.sun are also substantially faster; therefore the reader should ask, what benefits can be expected from using this new method? The previously demonstrated increase in predictive accuracy is only part of the answer to such a query.

In the authors' opinion there is equally increased value in having a full 3D model of a city. Foremost, detailed rooftop area information is available for quantifying useful rooftop area and the total incident irradiation (kWh) used in the energy generation equations. Such a model also provides opportunities to investigate wall mounted PV, and subsets of the model can easily be extracted to support further analysis by design teams or government entities that make policy. Solar installers may also benefit from having three-dimensional data for analysis in lieu of a site visit. Figure 10 illustrates the utility of this model in analyzing the solar potential of building walls. It shows that building walls annually receive between 200 and 1,200 kWh/m^2-yr of solar irradiation. Using a simple calculation of an efficiency factor – 18.5% – multiplied by irradiation, results in predicted photovoltaic energy production of between 37 and 222 kWh/m^2-yr. This means that some exposed building walls have the capacity of being ranked 'good' or 'excellent' for potential PV installations by the above criteria. Using the validated Daysim software provides additional confidence in the simulation results as it considers typical climate-based weather information, shading and reflections. As discussed, Daysim also provides access to hourly calculated irradiation data which facilitates the use of detailed equations of PV yield that consider hourly temperature predictions. Such hourly data can be used in policy analysis applications to help offset the peak loads of specific cities, areas or building types. For building owners who have a demand pricing arrangement, hourly predictive data is especially useful in reducing annual electricity costs. Demand pricing is an arrangement with an energy provider where the pricing structure for the entire year is determined based on peak usage. In such cases, it makes sense to optimize PV panel placement specifically for peak reduction using hourly or sub-hourly data.

Limitations of New Method

Beyond what was discussed previously, the new method has several limitations. Currently all PV panels are modeled as coincident with the roof; however, it is often the case that flat roofed buildings have PV panels installed at a 45 degree tilt towards the South using standardized angle brackets. Future solar maps should therefore consider an additional visualization layer with new simulation data analyzing potential photovoltaic installations tilted towards the South in this manner. Further, while the method produces reasonably accurate roof forms, it should be noted that LiDAR data and our point-simplifying method introduce errors in some buildings. A newer version of the map being produced uses finer resampling of the LiDAR data which results in significant improvements in geometric accuracy.

Others (Jochem et al. 2009, Levinson et al. 2009 and Lukač et al. 2012) have modeled the light passing through vegetation by using either fixed transmissivity percentages for the vegetative components of a DEM or through time-varying methods which account for the seasonality of leaf density. While our model does not currently implement such analysis, the Daysim software is capable of modeling time-varying object transmissivity by

changing physically-based material definitions during different times of the year. One limitation to implementing this over a large urban area such as a city or region is that existing GIS datasets rarely differentiate between deciduous and evergreen trees. Lukač et al. further note that surveying such information is only possible for small study regions. As GIS databases and remote sensing improve, modeling each tree explicitly will become possible.

CONCLUSION AND OUTLOOK

We have found that using a detailed Daysim reverse raytracing simulation at the scale of the city is feasible and produces reliable results. The new method employs detailed sky models based on measured climate data, considers reflections from the urban surroundings and includes an hourly rooftop temperature model. The capability of Daysim to accurately predict urban irradiation and the presented method to transform that irradiation into accurate PV energy yields is confirmed by a strong agreement between simulated and measured energy production at two PV installations in Cambridge where annual errors ranged from 3.6-5.3%. This error range was found to be smaller than variations in predicted electricity generation between separate years from 2008 to 2011.

Energy production predicted using the new method is often less than currently available maps would calculate for equivalent theoretical PV systems due to the urban rooftop temperature-based efficiency model. A validation study of a system located on the MIT student center building comparing panels nearly coincident with a roof surface suggests an average decrease in energy generation of 18.3% during the sunlit hours of a hot summer week through this effect and a peak decrease of 36.7% when the panel temperature is highest.

To validate irradiation models and predictions of photovoltaic energy generation at the urban scale is a new effort. We believe that in the future, such models will support policy decisions as they allow the ability to predict hourly peak-load reduction at the scale of a city or among a group of buildings whereas previous methods have not had this benefit. With increased model quality and certainty about results that can be – at least partially – visually assessed, the authors aim to increase public engagement with sustainable technologies.

REFERENCES

Bergamasco, L and Asinari, P. 2011. Scalable methodology for the photovoltaic solar energy potential assessment based on available roof surface area: Application to Piedmont Region (Italy). Solar Energy 85 (5): 1041-55.

Berkeley Solar Map. Retrieved on 3/5/2012 and 2/28/2013. http://berkeley.solarmap.org.

Brito MC, Gomes, N, Santos, T, Tenedório, JA. 2012. Photovoltaic potential in a Lisbon suburb using LiDAR data. Solar Energy. 86 (1): 283-8.

Cambridge, Massachusetts Weather. Retrieved on 07/21/2012. http://weather.keneli.org/index.html.

Cameron, CP, Boyson ,WE and Riley DM. 2008. Comparison of PV system performance-model predictions with measured PV system performance. Photovoltaic Specialists Conference, San Diego.

Choi, Y, Rayl, J, Tammineedi, C, and Brownson JRS. 2011. PV Analyst: Coupling ArcGIS with TRNSYS to assess distributed photovoltaic potential in urban areas. Solar Energy. 85 (11): 2924:39.

City of Anaheim Solar Map. Retrieved on 3/5/2012 and 2/28/2013. http://anaheim.solarmap.org.

City of Cambridge. GIS Buildings Layer. 2004. Retrieved on 1/15/2012. http://gis.cambridgema.gov/DataDictionary/Datapages/Buildings.html.

City of Cambridge. Property Database. 2011.

Daysim software. 2013. Version 4.0. Retrieved from http://daysim.ning.com/.

Denver Regional Solar Map. Retrieved on 3/5/2012 and 2/28/2013. http://solarmap.drcog.org.

DSIRESOLAR. 2012. Retrieved on 12/1/2012. http://www.dsireusa.org/solar/incentives/incentive.cfm?Incentive_Code=MA98F&re=1&ee=1.

Energy Improvement and Extension Act. Public Law 110-343. 122 Stat. 3807. 2008.

Fu, P and Rich, PM. 1999. Design and implementation of the Solar Analyst: an ArcView extension for modeling solar radiation at landscape scales. Proceedings of the Nineteenth Annual ESRI User Conference.

Geostellar. Retrieved on 2/28/2013. http://www.geostellar.com/.

GRASS Development Team. 2013. Geographic Resources Analysis Support System (GRASS), GNU General Public License.

Hofierka, J and Kaňuk, J. 2009. Assessment of photovoltaic potential in urban areas using open-source solar radiation tools. Renewable Energy. 34 (10): 2206-14.

Hofierka, J, Šúri, M and Huld, T. Grass GIS manual: r.sun. Retrieved on 2/21/2013. http://grass.osgeo.org/grass64/manuals/r.sun.html.

Huld, T, Šúri, M, Dunlop, ED and Micale, F. 2006. Estimating average daytime and daily temperature profiles within Europe. Environmental Modelling & Software. 21 (12): 1650-61.

Huld, T, Müller, R and Gambardella, A. 2012. A new solar radiation database for estimating PV performance in Europe and Africa. Solar Energy. 86 (6): 2012.

Ibarra, D. and Reinhart, CF. 2011. Solar availability: A comparison study of irradiation distribution methods. Proceedings of Building Simulation 2011, Sydney.

Jakubiec. JA and Reinhart, CF. 2012. The 'adaptive zone' - A concept for assessing glare throughout daylit spaces. Lighting Research and Technology. 44(2): 149-70.

Jochem, A, Höfle, B, Hollaus, M and Rutzinger M. 2009. Object detection in airborne LiDAR data for improved solar radiation modeling in urban areas. Proceedings of international archives of photogrammetry, remote sensing and spatial information sciences. v38. Paris.

King, DL, Quintana, MA, Kratochvil, JA, Ellibee, DE, Hansen, BR. 1998. Photovoltaic module performance and durability following long-term field exposure. National center for photovoltaics 15th program review meeting.

LA county Solar Map. Retrieved on 3/5/2012 and 2/28/2013. http://solarmap.lacounty.gov.

Levinson, R, Akbari, H, Pomerantz, M and Gupta S. 2009. Solar access of residential rooftops in four California cities. Solar Energy. 83 (12): 2120–35.

LiDAR Campaign (Boston) Report of Survey. 2010. Alliance for Sustainable Energy, LLC.

Lukač, N, Žlaus, D, Seme, S, Žalik, B and Štumberger, G. 2012. Rating of roofs' surfaces regarding their solar potential and suitability for PV systems, based on LiDAR data. Applied Energy. 102: 803-12.

Luque, A and Hegedus, S. 2011. Handbook of photovoltaic science and engineering, 2nd edition. John Wiley & Sons, Ltd.

MadiSUN. Retrieved on 3/5/2012 and 2/28/2013. http://solarmap.cityofmadison.com/madisun.

Mardaljevic, J. 2000. The simulation of annual daylighting profiles for internal illuminance. Lighting Research and Technology, 32(3): 111-8.

Marion, B, et al. 2001. PVWATTS version 2 -- Enhanced spatial resolution for calculating grid-connected PV performance. National Renewable Energy Laboratory publication NREL/CP-560-30941.

Massachusetts Clean Energy Center. Installers, Costs, Etc. Retrieved on 5/07/2012. http://masscec.com/masscec/file/Installers,%20Costs,%20Etc%20for%20Website%203-16-2012.xls.

Massachusetts Clean Energy Center. Commonweath Solar II. Retrieved on 5/07/2012. http://masscec.com/index.cfm/page/Commonwealth-Solar-II/cdid/11241/pid/11159.

Metro Orlando Solar Map. Retrieved on 2/28/2013. http://gis.ouc.com/solarmap/index.html.

Nguyen, HT and Pearce, JM. 2010. Estimating potential photovoltaic yield with r.sun and the open source Geographical Resources Analysis Support System. Solar Energy 84 (5): 831-43.

Nguyen, HT and Pearce, JM. 2012. Incorporating shading losses in solar photovoltaic potential assessment at the municipal scale. Solar Energy 86 (5): 1245-60.

NYC Solar Map. Retrieved on 3/5/2012 and 2/28/2013. http://nycsolarmap.com.

Oregon Clean Energy Map. Retrieved on 3/5/2012. http://oregon.cleanenergymap.com.

Our Green Community: Solar Map. Retrieved on 2/28/2013. http://smud.solarmap.org/.

Palmas, C, Abis, E, von Haaren, C and Lovett, A. 2012. Renewables in residential development: an integrated GIS-based multicriteria approach for decentralized micro-renewable energy production in new settlement development: a case study of the eastern metropolitan area of Cagliari, Sardinia, Italy. Energy, Sustainability and Society. 2 (10).

Perez, R, Seals, R and Michalsky, J. 1993. All-weather model for sky luminance distribution—Preliminary configuration and validation. Solar Energy 50 (3): 235-45.

Quintana, MA, King, DL, McMahon, TJ, Osterwald, CR. 2002. Commonly observed degradation in field-aged photovoltaic modules. Conference record of the 29th IEEE Photovoltaic Specialists Conference: 1436-9.

Reindl, DT, Beckman, WA, and Duffie, JA. 1990. Diffuse fraction correlations. Solar Energy 45 (1): 1-7.

Reinhart, CF and Walkenhorst, O. 2001. Validation of dynamic RADIANCE-based daylight simulations for a test office with external blinds. Energy and Buildings 33 (7): 683-97.

Reinhart, CF and Andersen, M. 2006. Development and validation of a Radiance model for a translucent panel. Energy and Buildings. 38 (7): 890-904.

Reinhart CF and Breton PF. 2009. Experimental Validation of Autodesk® 3ds Max® Design 2009 and Daysim3.0. Leukos. 6 (1).

Renew Boston Solar. Retrieved on 3/5/2012 and 2/28/2013. http://gis.cityofboston.gov/SolarBoston/.

Renewable Energy Property Tax Exemption. Massachusetts General Law. Ch. 59 §5 (45, 45A). 1975.

Residential Renewable Energy Income Tax Credit. Massachusetts General Law. Ch. 62. §6(d). 1979.

Rich, PM, Dubayah, R, Hetrick, WA and Saving, SC. 1994. Using viewshed models to calculate intercepted solar radiation: applications in ecology. American Society for Photogrammetry and Remote Sensing Technical Papers. 524-9.

Robinson, D and Stone, A. 2004. Irradiation modelling made simple: the cumulative sky approach and its applications. Plea 2004 – The 21st Conference on Passive and Low Energy Architecture, Eindhoven.

Ruiz-Arias, JA, Tovar-Pescador, J, Pozo-Vazquez, D, Alsamamra, H. 2009. A comparative analysis of DEM-based models to estimate the solar radiation in mountainous terrain. International Journal of Geographical Information Science. 23 (8): 1049–76.

Ruiz-Arias, JA, Terrados, J, Pérez-Higueras, P, Pozo-Vázquez, D and Almonacid, G. 2012. Assessment of the renewable energies potential for intensive electricity production in the province of Jaén, southern Spain. Renewable and Sustainable Energy Reviews. 16: 2994-3001.

Rtrace man page. Retrieved on 7/1/2012. http://radsite.lbl.gov/radiance/man_html/rtrace.1.html.

Salt Lake City Solar. Retrieved on 3/5/2012 and 2/28/2013. http://slcgovsolar.com.

San Diego Solar Map. Retrieved on 3/5/2012 and 2/28/2013. http://sd.solarmap.org/solar/index.php.

San Francisco Solar Map. Retrieved on 3/5/2012 and 2/28/2013. http://sf.solarmap.org.

Schallenberg-Rodriguez, J. 2013. A methodological review to estimate techno-economical wind energy production. Renewable and Sustainable Energy Reviews. 21: 272-87.

Schwarz, C and Wade, E. 1990. The North American datum of 1983: Project methodology and execution. Journal of Geodesy 64 (1): 28-62.

Sunpower E18/230 Solar Panel Technical Sheet. Retrieved on 3/1/2012. http://us.sunpowercorp.com/cs/BlobServer?blobkey=id&blobwhere=1300258626946&blobheadername2=Content-Disposition&blobheadername1=Content-Type&blobheadervalue2=inline%3B+filename%3Dsp_230wh_en_ltr_w_ds.pdf&blobheadervalue1=application%2Fpdf&blobcol=urldata&blobtable=MungoBlobs.

Šúri, M and Hofierka, J. 2004. A New GIS-based Solar Radiation Model and Its Application to Photovoltaic Assessments. Transactions in GIS. 8(2): 175–90.

Šúri, M, Huld, TA, Dunlop, ED. 2005. PV-GIS: a web-based solar radiation database for the calculation of PV potential in Europe. International Journal of Sustainable Energy. 24 (2): 55-67.

United States Department of Energy. EnergyPlus Weather Data. Retrieved on 2/1/2012. http://apps1.eere.energy.gov/buildings/energyplus/cfm/weather_data.cfm.

Yimprayoon, C and Navvab, M. 2010. Quantification of available solar irradiation on rooftops using orthophotograph and LiDAR data. SimBuild 2010: Proceedings of the Fourth National Conference of IBPSA-USA.